JOURNAL OF Materials CHEMISTRY

Chiral hexacatenar metallomesogens: supramolecular organization *versus* steric demand of chiral cores

Matthias Lehmann,[a]† Teresa Sierra,[a] Joaquin Barberá,[a] José Luis Serrano*[a] and Robert Parker[b]

[a]*Química Orgánica, Facultad de Ciencias-I.C.M.A., Universidad de Zaragoza-C.S.I.C., 50009 Zaragoza, Spain. E-mail: joseluis@posta.unizar.es*
[b]*BASF Aktiengesellschaft, Specialty Chemicals Research, 67056 Ludwigshafen, Germany*

Received 18th October 2001, Accepted 25th January 2002
First published as an Advance Article on the web 14th March 2002

Hexacatenar chiral oxazoline complexes were prepared in a stereospecific synthesis. Metals (Pd, Ni, Cu, Zn), lateral alkoxy chains (OC_6H_{13}, $OC_{12}H_{25}$), sterically demanding alkyl groups (CH_3, C_4H_9) on the chiral rigid centre and the number of nuclei incorporated in the complex core (mononuclear, orthopalladated dinuclear) were varied in order to achieve supramolecular organization of the phasmid-like molecules in liquid crystal phases. Mesomorphic properties were not observed in neat materials, but phase diagrams of binary mixtures with TNF demonstrate that steric repulsion can be overcome by intercalation of the electron-acceptor TNF. In spite of the presence of six lateral chains, SmA phases were found exclusively. The structures of the SmA phases were found to have additional order with respect to SmA phases formed by calamitic molecules. Further examination of the complexes in host nematic materials demonstrated their use as chiral dopants to induce cholesteric LC phases.

Introduction

Self-organization in condensed matter is an essential feature for many applications in materials chemistry including liquid crystal displays, data storage devices and chemical sensors. The supramolecular chemistry of chiral molecules has attracted our attention because of their ferroelectric properties and, consequently, their applicability in switchable mesophases or in dielectric data storage devices.[1]

It has recently been demonstrated that chiral oxazolines organize in monotropic cholesteric and chiral smectic C mesophases.[2] On doping achiral smectic hosts with these materials, ferroelectric phases were obtained with large spontaneous polarization values. Complexation of the monocatenar ligands to metals like copper(II) or palladium(II) results in smectic A mesophases.[3] Encouraged by this observation we decided to investigate this area and proposed the general structure **1** (Chart 1) to be phasmid-like, with C being a central complexing unit. Such rod-like polycatenar molecules are known to form either smectic or columnar self assemblies.[4] Liquid crystal phases formed by chiral discotic or smectic mesogens are well known and electrooptical switching has been demonstrated. Chirality was introduced within the peripheral chains of these systems.[5] In contrast, we have chosen a molecular architecture in which the central rigid oxazoline ring bears the chiral unit. The question of self-organization of these molecules was envisaged to be a possible problem because of the presence of the sterically demanding core of complexes **1**. In the following contribution we report on the synthesis of phasmidic metallomesogens **1** bearing chirality in the centre of the core, the thermal properties of these compounds as neat materials, their organization in mixtures with the electron-acceptor trinitrofluorenone (TNF) and their potential as chiral dopants in nematic mesophases.

†*Current address*: Laboratoire de Chimie des Polymères CP206/1, Université Libre de Bruxelles, Boulevard du Triomphe, 1050 Bruxelles, Belgium.

Synthesis

The general stereospecific route to enantiomerically pure oxazolines **4a–c** is shown in Scheme 1.[2,6] The alkoxy chains were introduced *via* the polycatenar acid chlorides **5**. Coupling of acid chlorides **5** with phenols **4a–c** gave the chiral polycatenar ligands **2a–e**. The complexes **1a–m** were formed by the reaction of ligands **2a–e** with the corresponding metal acetates. The binuclear chloride-bridged compounds **1n** were obtained by exchange of the acetato-bridge with chloride by reaction with one equivalent of HCl[7] (Scheme 2)

^1H and ^{13}C NMR spectroscopy confirmed the two-fold symmetry of the final products. Table 1 summarizes the ^1H NMR data of ligands and complexes bearing dodecyloxy side

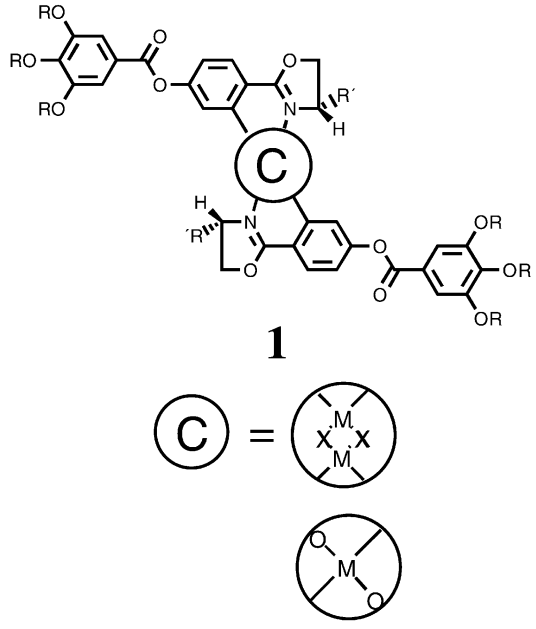

Chart 1

 DOI: 10.1039/b109487d

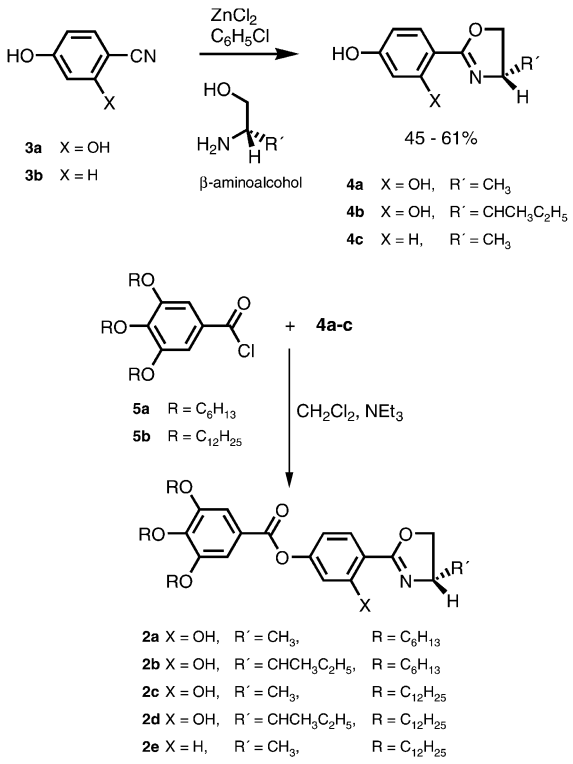

Scheme 1 Stereospecific synthesis of chiral oxazoline ligands.

chains and a methyl group at the stereogenic centre. The signals due to the peripheral gallic acid moiety (aA peripheral aromatic protons, OCH_2) are generally not affected by complexation. The metal does, however, influence the chemical shifts of the oxazoline protons (ox) and the protons corresponding to the inner aromatic benzene ring (iA). The signals observed for the free ligands could not be observed in the spectra of the final complexes. Signals corresponding to the *anti*-stereoisomer were found exclusively for the dinuclear acetato-bridged complex **1m**, whereas the ^{1}H NMR spectrum of the chloro-bridged complex **1n** shows signals that are due to a mixture of *syn*- and *anti*-isomers.[3,6c]

The copper complexes could not be analysed by NMR methods due to the paramagnetic nature of the metal. These complexes were characterised by means of elemental analysis, FT-IR spectroscopy and mass spectrometry. The FT-IR spectra of all the complexes show that free ligand is not present in the recrystallised materials. The signal corresponding to the C=N double bond of the free ligands (1643–1649 cm^{-1}) is shifted to lower frequencies by about 20 cm^{-1} in the spectra of the complexes (1620–1633 cm^{-1}).[6,8] In general, the FAB mass spectra of the complexes contain predominantly fragment signals due to the benzoyl ester (m/z = 490, 658 for dodecyloxy chains or m/z = 321, 405 for hexyloxy chains). Molecular ion peaks are small and often have similar intensities as $[M + Na]^+$, $[M - ligand]^+$, $[ligand]^+$ and the cluster peak $[2M - ligand]^+$. Characteristically for copper complexes, the signals for $[M + Cu]^+$ ions are observed to be greater in intensity than the molecular ion peaks. This fact could be due to the

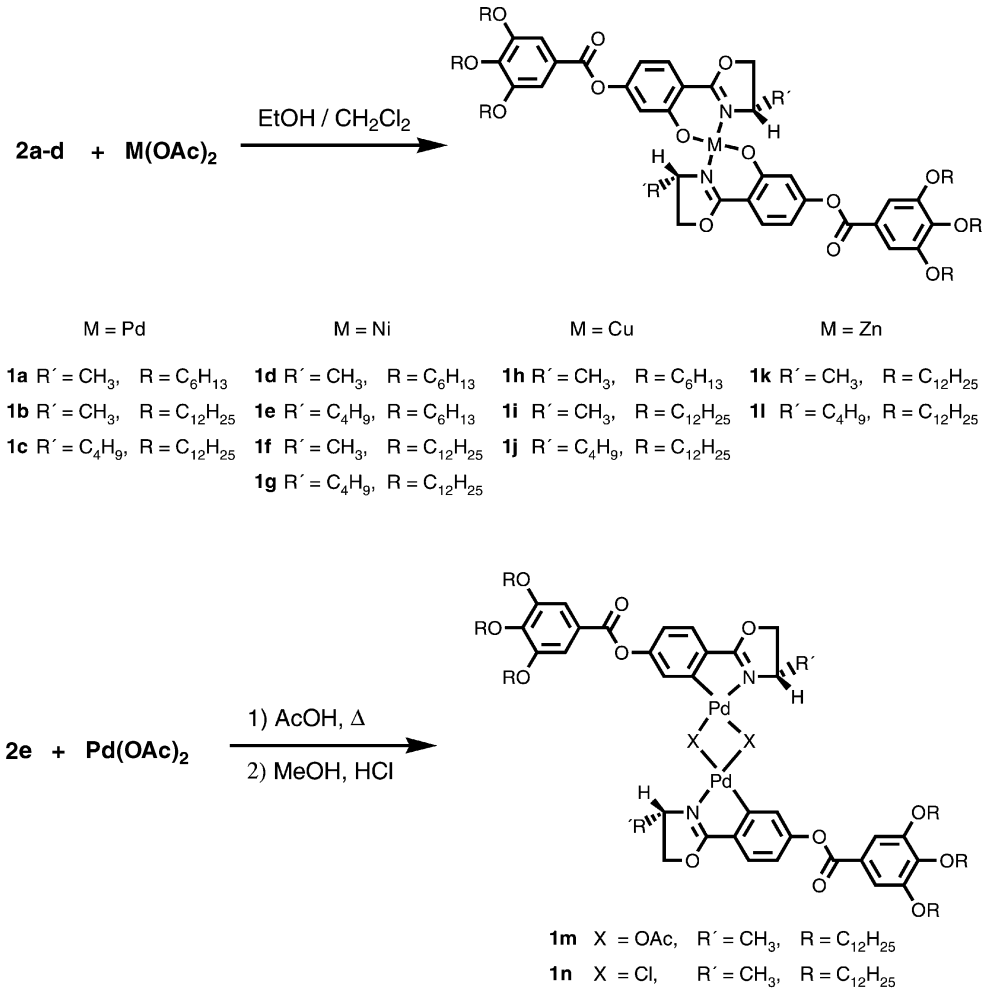

Scheme 2 Synthesis of chiral hexacatenar complexes.

Table 1 ^{1}H NMR data of oxazoline complexes δ [ppm] in $CDCl_3$ with TMS as an internal standard

Complexes	aA[a]	iA[a]	ox[a]	OCH_2	OH
2c	7.39	7.69; 6.87; 6.74	4.49; 4.45; 3.96	4.07; 4.05	12.45
2d	7.39	7.68; 6.87; 6.74	4.43; 4.25; 4.13	4.07; 4.05	12.60
2e	7.39	8.02; 7.25	4.55; 4.40; 3.98	4.06; 4.04	
1b	7.37	7.64; 6.66; 6.42	4.59; 4.29	4.05; 4.03	
1f	7.39	7.49; 6.39; 6.32	4.41; 4.15; 4.09	4.04; 4.02	
1k	7.35	7.74; 6.67; 6.44	4.61; 4.45	4.04; 4.05	
1m	7.37	7.14; 6.92; 6.83	3.98; 3.95; 3.55	4.05	
1n	7.38	7.22; 7.14; 6.91	4.77; 4.31	4.04	

[a]**aA** peripheral aromatic protons, **iA** inner aromatic protons, **ox** oxazoline protons.

preformation of dimers, a phenomenon that was observed by Bolm *et al.* in the single crystal of similar copper complexes.[6]

Results and discussion

Thermal behaviour of neat samples

The thermal behaviour of the neat oxazoline complexes was investigated by means of differential scanning calorimetry and optical microscopy. The results are summarised in Table 2.

Three parameters were systematically varied in an attempt to achieve supramolecular phasmid-like assemblies of the hexacatenar complexes: (i) length of the peripheral alkoxy chains, (ii) size of the substituent on the stereogenic centre, (iii) size and geometry of the central part of the complex. In the series of monocatenar oxazoline ligands the 2-methylpropyl substituent at the stereogenic centre stabilises a smectic arrangement, whereas the phasmidic complexes (**1c**, **1e**, **1g**, **1j**) form amorphous materials that, in some cases, partially crystallise over a long period of time. The Zn complex **1l** crystallises with a slow heating rate, which is due to the geometry of the complex and will be discussed below. Complexes with hexyloxy chains (**1a**, **1d**, **1e**, **1h**) are glassy or oily materials. The combination of a small substituent at the stereogenic centre (methyl) and long peripheral chains (dodecyloxy) (**1b**, **1f**, **1i**, **1k**, **1l**, **1m**, **1n**) results, in some cases (**1f**, **1i**, **1k**, **1l**), in crystalline phases. In the different metal oxazoline complexes, it is known that changing the metal through the series Pd, Ni, Cu to Zn leads to a change in the geometry of the molecules from a planar arrangement to a tetrahedral geometry. Regardless of the metal, the substituents at the stereogenic centres point to the same side of the molecule in all of the complexes.[6] The DSC data of complexes **1** show that deviation from a planar conformation allows crystallisation even for complexes with sterically demanding 2-methylpropyl groups such as, for example, the zinc complex **1l**. Thus, the alkyl groups on the stereogenic centre inhibit the arrangement of the molecules in stacks and crystallisation is even prevented for the planar complex configuration. The enlargement of the central core unit caused by preparing the dinuclear complexes **1m** and **1n**, which provides additional free space to minimise the steric repulsion of the molecules, results in amorphous solids. Liquid crystal phases were not observed in the neat materials.

Table 2 DSC data for the complexes **1** at a heating rate of 10 °C min^{-1}

Complex	Second heating T[°C]/ΔH [kJ mol^{-1}]
1a	g 22(T_g) I[b]
1b	g 22(T_g) I[b]
1c	g 34(T_g) I
1d	Oil[a]
1e	g 28(T_g) I[b]
1f	Cr 69/16 I
1g	g 8(T_g) I[c]
1h	g 44(T_g) I
1i	Cr 88/17 I
1j	g 24(T_g) I[c]
1k	Cr 94/16 I[d]
1l	Cr1 25/12 Cr2 55/8 I
1m	Oil[c]
1n	g 67(T_g) I

[a]No transition in DSC curves. [b]Metastable crystals after preparation, melting transitions were only observed in the first heating cycle. [c]Partial crystallisation within hours/days. [d]Heating rate: 2 °C min^{-1}.

Thermal behaviour of the mixtures with TNF

It is well known that charge transfer interactions with electron acceptors like TNF stabilise LC phases.[9] The influence of TNF charge transfer interactions on different planar complexes has already been investigated.[10,11] A weak charge transfer and quadrupolar interactions were found to stabilise SmA phases. In studies with phasmidic mesogens ''filled SmA phases'' were observed.[12] Thus, intercalation of TNF could primarily reduce steric repulsive forces between complexes **1** as well as stabilise the supramolecular array by electronic interactions. We therefore investigated the phase behaviour of complex–TNF mixtures by means of the contact method and by DSC studies of mixtures with known concentrations. All compounds **1** form a charge transfer complex with TNF, which was evidenced by a colour change to reddish brown in the contact region. Compounds **1b** and **1c** were chosen for a more detailed investigation. These two planar complexes differ only in the size of the alkyl group at the stereogenic centre. Compound **1c** should provide more space for the intercalation of TNF. Tables 3 and 4 show the behaviour of both binary mixtures and these are based on the DSC data of the second heating curve obtained with a heating rate of 10 °C min^{-1}. A high tendency for component separation can be observed for both mixtures at high TNF concentrations ($>$ 66%). In these mixtures SmA phases were found in addition to crystalline phases of both TNF and mixtures of TNF with complexes **1b**,**c**. Fig. 1 shows the texture of the mixture **1b** : TNF = 1 : 2 and it can be seen that this is a typical fan texture observed for SmA phases. The SmA phases are only metastable in these high concentration regions of TNF. Cooling the sample at a slow rate (*e.g.* 5 °C min^{-1}) results in demixing and crystallisation of the material before reaching the temperature range at which the LC mesophases exist. Even the **1c**–TNF mixture that forms the SmA phase below 80 °C requires a cooling rate of 20 °C min^{-1} to prevent crystallisation. Once the smectic phases of **1c**–TNF have arranged they undergo a transition to smectic glasses close to 25 °C. SmA phases formed by mixtures of **1b** with TNF tend to crystallise to give Cr_{S2} even at temperatures above the corresponding transition in Table 4. This fact could be due to the lower repulsive steric interactions caused by the methyl groups in **1b** in comparison to the sterically demanding 1-methylpropyl group in **1c**, and to the possibility of an increased attractive interaction once TNF has been intercalated between two complexes. On heating the samples **1b**–TNF and **1c**–TNF above the clearing temperatures, a crystalline phase Cr_2 forms slowly and then begins to melt between 130–170 °C. Melting transitions in the DSC curves are not observed for these phases and they seem not to be

Table 3 Phase transitions of the binary mixtures **1c**–TNF. Data (onset temperatures in °C) were obtained from the second heating curve at a heating rate of 10 °C min^{-1}

1c–TNF [mol% TNF]	g	T_g/°C	Cr_1	SmA	T_{Cl}/°C[a] (SmA)	Cr_2[a]	Cr_{TNF}	T/°C	I
100							●	175	●
90						●			●
							○[b]	172	○[b]
75	●	20		●	77	●			●
							○[b]	173	○[b]
						□[b]			□[b]
66	●	23		●	69	●			●
							○[b]	174	○[b]
			□[b]		50	□[b]			□[b]
60	●	24		●	62				●
50	●	26		●	43				●
45	●	24		●	35				●
30	●	29							●
10	●	33							●
0	●	34							●

[a]After clearing of the SmA phase the Cr_2 phase grows up to 120 °C, then it slowly melts from 130–174 °C; a transition can not be observed in the DSC heating curve. This is most probably due to a partial separation of the components. [b]Coexisting phases: ○ coexisting TNF crystalline phase; □ coexisting crystalline phases Cr_1, Cr_2; in the cooling process, crystalline domains were growing before the temperature could be reached where the SmA phase exists.

Table 4 Phase transitions of the binary mixtures **1b**–TNF. The data (onset temperatures in °C) were obtained from the second heating curve at a heating rate of 10 °C min^{-1}

1b–TNF [mol% TNF]	g	T_g/°C	Cr_1/Cr_{S1}[a]	T/°C	Cr_{S2}[a]	T/°C	SmA	T_{Cl}/°C[b] (SmA)	Cr_2[b]	Cr_{TNF}	T/°C	I
100										●	175	●
90			●	80	●	96	●	98	●			●
										○[c]	174	○[c]
			□[c]	47					□[c]			□[c]
75		20	●	80	●	93	●	105	●			●
										○[c]	174	○[c]
			□[c]	42					□[c]			□[c]
66					●	91	●	109	●			●
60	●	22					●	44	●[d]		77	●
50	●	23										●
25	●	31										●
0	●	20[e]										●

[a]Crystal phases forming on cooling from the SmA phase. [b]After the clearing of the SmA phase, the Cr_2 phase grows up to 120 °C, then it melts slowly from 130–174 °C; a transition can not be observed in the DSC heating curve. This is most probably due to a partial separation of the components. [c]Coexisting phases: ○ coexisting TNF crystalline phase; □ coexisting crystalline phases Cr_1, Cr_2; in the cooling process, crystalline domains were growing before the temperature could be reached where the SmA phase exists. [d]The SmA phase recrystallises to a crystalline phase which is different from the Cr_2 phase mentioned in footnote *a*. [e]Data obtained from the first cooling curve.

homogenous. This situation is probably due to a partial separation of the components.

At low TNF contents, on the other hand, the mixtures show only glass transitions. In these cases separation of TNF and metal complexes was not observed. The most interesting mixture compositions are those with a TNF content of 45–60% for **1c**–TNF and 60–66% for **1b**–TNF. The mixtures are homogeneous and a transition for TNF was not found in the DSC curves. The **1b**–TNF mixture with 66% TNF still shows phase behaviour similar to mixtures with higher concentrations of the electron-acceptor, but with a larger temperature range of the mesophase. In contrast, the **1b**–TNF mixture with 60% TNF shows a smectic phase at a temperature as low as 53 °C (cooling curve). However, unlike the mixtures with 66% TNF, the higher viscosity prevents the material from crystallising and, on further cooling, a smectic glass is formed. Crystallisation occurs above the glass transition in the heating cycle.

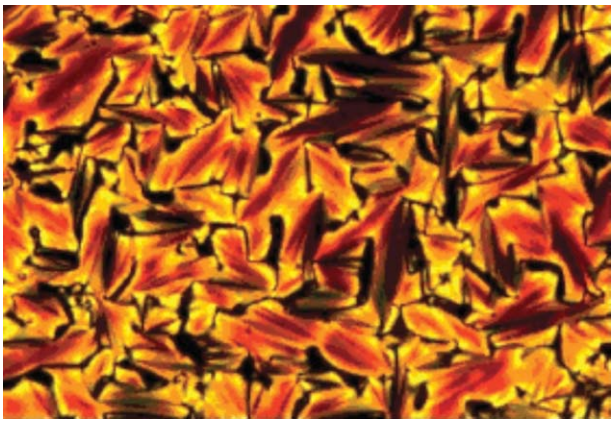

Fig. 1 Texture of mixture **1b** : TNF = 1 : 2 in the SmA phase at 85.2 °C, between crossed polarizers, obtained by cooling at 10 °C min^{-1}.

The mixtures **1c**–TNF form enantiotropic mesophases when the TNF contents are in the range 45–60%. Fig. 2 shows the texture of a 1 : 1 mixture, which cannot be unambiguously assigned as a SmA phase. LC glasses are formed close to room temperature. The temperature ranges of the mesophase continuously increase with increasing TNF concentration. Indeed, discontinuities were not found in this trend even in mixtures with high proportions of TNF (>60%)—where SmA phases were observed. X-Ray investigations on the 1 : 1 mixture **1c**–TNF (see below) provide evidence for a smectic A arrangement. Thus, this is an indication that all materials **1c**–TNF containing 75–45% TNF form SmA phases.

X-Ray studies

An X-ray diffraction study was carried out on two mixtures: **1b**–TNF in a ratio of 1 : 2 (TNF content 66%) and **1c**–TNF in

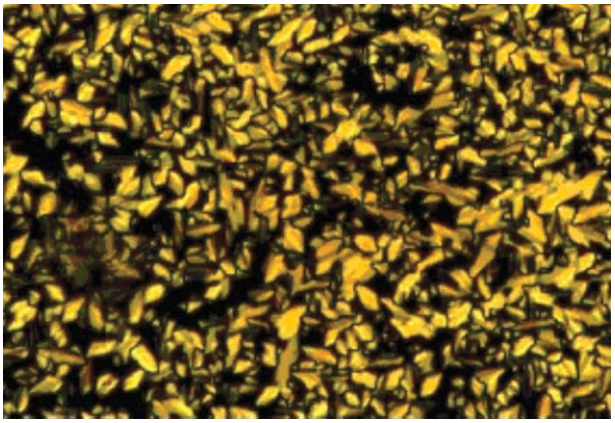

Fig. 2 Texture of mixture **1c**–TNF = 1 : 1 in the mesophase at 50.9 °C, between crossed polarizers, obtained by cooling at 10 °C min^{-1}.

a ratio 1 : 1 (TNF content of 50%). Patterns were initially taken at room temperature on as-prepared mixtures and, subsequently, patterns were also taken after thermal treatment. This thermal treatment consisted of heating the Lindemann glass capillary containing each sample in an oven at a temperature high enough to give the isotropic liquid and then cooling the sample to room temperature.

The X-ray pattern taken on the as-prepared mixture **1b**–TNF (1 : 2) contains a number of sharp rings that are not consistent with a liquid crystal phase and indicate that the sample either is completely crystallised or contains a significant amount of a crystalline phase. On the other hand, the as-prepared mixture **1c**–TNF (1 : 1) yielded a pattern characteristic of a liquid crystal phase. This pattern contains a set of two sharp maxima at small angles, the first of which is much stronger than the second. By applying Bragg's law, the deduced spacings are 42.5 Å and 14.2 Å. The fact that the spacing ratio is 1 : $\frac{1}{3}$ is consistent with a lamellar order, and these maxima are then assigned to the first and third order reflections from the layers. The absence of other reflections and the presence of only diffuse scattering in the middle and large angle regions supports the liquid crystal nature of this phase. These features are consistent with the assignment of the phase as smectic A, which was also made on the basis of the observations by optical microscopy. However, the presence of several diffuse rings suggests that this mesophase is not a conventional smectic A phase. Indeed, in addition to a diffuse ring found at about 4.5–4.6 Å, which is typically observed in all kinds of mesophases and is characteristic of the interferences between the conformationally-disordered hydrocarbon chains, diffuse maxima are observed at about 20 Å, 10 Å and 3.7 Å. The presence of this scattering pattern indicates that there is some kind of additional order that is usually absent in a smectic A mesophase.

The same pattern is obtained when this sample is studied at room temperature after the same thermal treatment as described above. This fact demonstrates that the mixture **1c**–TNF (1 : 1) adopts a smectic A arrangement at room temperature regardless of its previous thermal history.

In contrast, mixture **1b**–TNF (1 : 2) adopts a crystalline structure, not only before any thermal treatment but also after the sample has been slowly cooled from the isotropic liquid to room temperature. However, when the X-ray study was performed on a quenched sample (a sample quickly cooled from the isotropic liquid), a pattern consistent with a smectic A mesophase was obtained that was similar to the one found for the mixture **1c**–TNF (1 : 1). This pattern contains a sharp maximum characteristic of layer stacking with a spacing of 42.5 Å, as well as three broad, diffuse rings corresponding to distances of about 9–9.5 Å, 4.4 Å and 3.6 Å. In this case, neither high order reflections from the layers nor diffuse scattering at about 20 Å are observed.

It is worth noting that the measured layer thickness is the same for both mixtures (42.5 Å). This situation is expected as **1b** and **1c** have exactly the same length—the only difference between them being the central core.

Further insight into the structure of the mesophases exhibited by these mixtures can be obtained from oriented patterns. With this aim in mind, aligned samples were prepared by spreading the samples on the surface of the internal wall of the Lindemann capillaries and, upon cooling from the isotropic liquid into the smectic mesophase, using a metal or glass rod to "scratch" in the direction of the capillary axis.

A well-oriented pattern was obtained for mixture **1c**–TNF (1 : 1). Several features can be distinguished in this pattern (Fig. 3):

(1) Two pairs of spots are observed in the direction perpendicular to the capillary axis (spots along the meridian in Fig. 3, denoted **a**), the first of which is much stronger than the second. These spots appear at the same diffraction angles as the two small-angle maxima observed for the non-aligned mixture **1c**–TNF (1 : 1) (see above). Thus, the spots correspond to the first and third order reflection from the smectic layers and give a layer spacing of 42.5 Å. The X-ray reflections from a lamellar structure occur along the normal to the lamellae and, therefore, in this case the pattern indicates that the layer normals are perpendicular to the capillary axis; *i.e.* the smectic layers are parallel to the glass walls (homeotropic alignment).

(2) At middle and large angles, the diffuse scattering is centred in the direction of the capillary axis (equator in Fig. 3). This is especially true for the maximum corresponding to about 20–21 Å (denoted **b**), which appears as a pair of arcs. On the

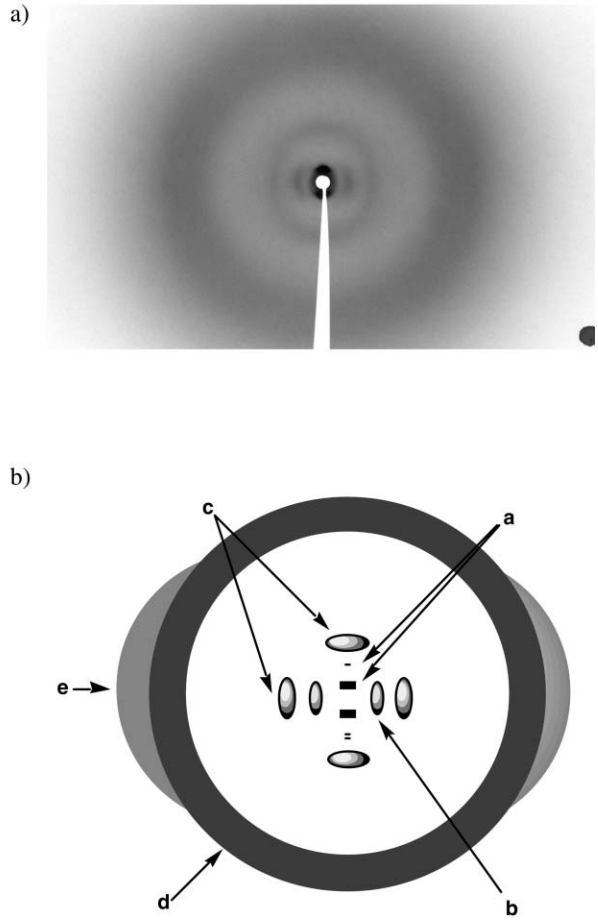

Fig. 3 a) X-Ray photograph of **1c**–TNF (1 : 1). b) Schematic drawing of photograph in a).

other hand, the diffuse maximum at about 4.5 Å (denoted **d**), which is related to the disordered hydrocarbon chains, is rather isotropic, *i.e.* does not show any preferred direction, indicating poor orientation of the chains. The intensity of this maximum is reinforced at the large-angle side, where a shoulder is observed at about 3.7 Å (denoted **e**). This reinforcement is more visible near the equator and, therefore, this maximum, along with that at 20–21 Å, is related to some kind of short-range positional order within the layers.

In addition to the features described above, a diffuse shell with an elliptical shape (denoted **c**) is seen at middle angles, and the intensity of this shell is concentrated in the directions of the meridian and equator. The scattered intensity centred in the equator corresponds to a distance of about 10–11 Å and must be associated with the existence of interactions within the smectic layers. The intensity scattered in the meridian corresponds to a distance of about 9–10 Å and is associated with interactions along the molecular director. This elliptical scattering has been observed in pure mesomorphic palladium complexes,[13] and the phenomenon has been assigned to the existence of local order arising from the peculiar shape of these molecules. In particular, the scattering observed in the equator can be related to the mean lateral distance between two neighbouring molecules arranged side by side. The scattered intensity observed in the meridian in this kind of metallomesogen can be accounted for by a mutual shifting of neighbouring molecules inside each layer in the direction of the main molecular axis. Thus, adjacent molecules lie parallel to each other in a side-by-side arrangement, but the palladium atoms tend to lie on each side of the median plane of the layer at a distance of 4.5–5 Å from that plane.

The scattering corresponding to 3.7 Å may be due to the intermolecular face-to-face distance. This distance is slightly longer than the value of about 3.4 Å that is typical for face-to-face distances in other aromatic π–π systems. However, we must take into account the fact that, in the complexes described in the present paper, the central part of the molecule is not completely flat and is sterically hindered.

Based on the features discussed above we can propose that the layers are formed by a mixture of palladium complexes and TNF molecules stacked in a face-to-face manner. The 20–21 Å spacing would be the lateral distance between two palladium complexes separated by a TNF molecule. The molecules are orthogonal to the layer planes and there is an additional short-range side-by-side organization. This structure resembles that proposed by Tschierske and coworkers[11] for other binary systems of a palladium-containing metallomesogen and TNF, which was described by the same authors as a McMillan phase.[14]

Although attempts to obtain a well-oriented pattern of mixture **1b**–TNF (1 : 2), using the method applied for mixture **1c**–TNF (1 : 1), were not successful, a partially-oriented pattern could be obtained. In this pattern the small-angle maximum at 42.5 Å transforms into an arc centered in the direction perpendicular to the alignment direction. This indicates that the layers lie parallel to the surface of the glass capillary (homeotropic alignment) as in mixture **1c**–TNF (1 : 1). Some diffuse intensity scattered at 9–9.5 Å, 4.4 Å and 3.6 Å is also visible. However, because of the poor orientation of the sample, these rings do not show any preferred direction. No other scattered intensity is observed. It can be concluded that the structure of the smectic A mesophase of this mixture is similar to that of mixture **1c**–TNF (1 : 1). There are, however, two significant differences: instead of a face-to-face arrangement containing one TNF molecule per palladium complex, in mixture **1b**–TNF (1 : 2) each palladium complex alternates with two TNF molecules. Furthermore, the smaller degree of steric hindrance of the central core of **1b** compared to **1c** allows for a slightly closer face-to-face arrangement.

Table 5 Helical twisting power (HTP) measured by the Cano Method in the nematic Paliocolor® LC242,[16] commercially available from BASF-Aktiengesellschaft, Ludwigshafen, Germany

Complex	HTP/μm^{-1}
1a	30
1d	20
1e	15
1f	<2
1g	<2
1h	30

Use as chiral dopants for cholesteric LC phases

To further probe the chiral information held within the central rigid oxazoline ring, the ability of certain complexes to act as chiral dopants and to induce a cholesteric LC phase in a host nematic phase was examined through the measurement of the helical twisting power (HTP).[15] In particular, **1a**, **1d**, **1e**, **1f**, **1g** and **1h** were chosen to reflect the different metal complexes, the variation in the peripheral alkoxy chains and the choice of stereogenic centre. The results are listed in Table 5.

The results indicate that the hypothesis that such complexes can induce a cholesteric phase is in part true. Indeed, there is a definite division in their efficiency—those that do induce a cholesteric phase contain peripheral chains with 6 carbon atoms (**1a**, **1d**, **1e**, **1h**); those that do not induce a cholesteric phase contain peripheral chains with 12 carbon atoms (**1f**, **1g**). This trend is primarily related to the compatibility of the dopant with the nematic phase, although it should be noted that those complexes with a 12-carbon peripheral chain are less soluble, but not insoluble, in the nematic phase than the 6-carbon containing derivatives.

Furthermore, it appears that the methyl-containing compounds (**1a**, **1d**, **1h**) exhibit a greater affinity for the nematic phase, as opposed to the 2-methylpropyl derivative (**1e**), and thereby induce a cholesteric phase with a higher HTP value—a similar effect to that seen with the TNF charge-transfer complexes.

It appears that the induction of a cholesteric phase is not influenced by the choice of the metal.

Conclusions

The stereospecific synthesis of hexacatenar, chiral oxazoline complexes has been demonstrated. The stereogenic centres are located in the core of the molecule. Thus, the sterically demanding alkyl groups prevent the molecules from organising in liquid crystalline phases, even for the dinuclear complexes **1m** and **1n**, which provide more space in the central part. Crystallisation is not observed unless the complexes deviate strongly from planarity, possess long alkyl chains and the smallest substituent (methyl group) at the stereogenic centre, as in the case of Cu, Ni and Zn complexes (**1f**, **1i**, **1k**). Steric factors can be overcome by intercalation of TNF, which leads to the formation of SmA phases. The sensitive balance between attractive and repulsive forces to build LC-phases is demonstrated by the fact that SmA phases formed by mixtures **1b**–TNF, *i.e.* with the less sterically demanding methyl group, crystallise rapidly. In stark contrast, the sterically demanding 1-methylpropyl groups in **1c**–TNF prevent the LC-phases from crystallising and stabilise the SmA phases over a larger temperature interval. X-Ray investigations show that the layers are formed by a mixture of palladium complexes and TNF molecules stacked in a face-to-face arrangement. Moreover, there is an additional short-range side-by-side organization within the layers, which resembles the structure previously proposed as a McMillan phase by Tschierske and coworkers.[11] Despite the presence of six lateral dodecyloxy chains, phases other than smectic ones were not observed in the binary

mixtures. Upon further investigation, it has been shown that when the compatibility with a host nematic phase is sufficiently great (*i.e.* the complex is soluble), the metal complexes can act as chiral dopants and induce a cholesteric liquid crystalline phase.

Experimental

General procedure for the preparation of ligands 2

The stereospecific route to oxazolinylphenols **2** is given in reference 2. To a solution of phenyloxazoline **4** (1.04 mmol) and acid chloride **5** in dry CH_2Cl_2 (40 ml) was added triethylamine (120 mg). The mixture was stirred for 24 h and filtered over silica. The solvent was evaporated and the residue was purified by column chromatography (silica gel 60, hexane–ethyl acetate).

General procedure for the preparation of the metal complexes

To a mixture of oxazoline ligand (0.4 mmol) and $M(OAc)_2 \cdot xH_2O$ (M = Pd, Ni, Cu, Zn) (0.2 mmol) was added dry ethanol (10 ml). The mixture was stirred for 5 min and CH_2Cl_2 (10 ml) was added to give a solution. The mixture was stirred for a further 30 min and the solvent was evaporated. The resulting solid was dissolved in acetone (10 ml) and ethanol (10 ml) was added. The volume of the solution was reduced to 10 ml. The product was crystallised or precipitated at ambient temperature.

(4*S*)-4,5-Dihydro-4-methyl-2-{4′-[3″,4″,5″-tris(hexyloxy)benzoyloxy]-2′-hydroxyphenyl}oxazole (2a). The general procedure gave **2a** as a colourless oil, yield 86%.

^{1}H NMR ($CDCl_3$, 300 MHz) 0.90 (m, 9H, CH_3), 1.34, 1.48, 1.79 (m, 27H, CH_2, CH_3), 4.04, 4.06 (t, 6H, OCH_2), 3.98, 4.48, 4.53 (m, 3H, oxazoline), 6.74, 6.89, 7.69 (m, 3H, inner Ar-H), 7.39 (s, 2H, outer Ar-H), 12.39 (s, 1H, OH). ^{13}C NMR ($CDCl_3$, 75 MHz) 14.0, 21.4 (CH_3), 22.6, 25.7, 29.2, 30.3, 31.5, 31.7 (CH_2), 60.6, 69.3, 73.4, 73.6 (OCH_2, oxazoline), 108.5, 108.6, 110.2, 112.6, 123.6, 128.9, 143.1, 153.0, 155.0, 161.2, 164.5, 164.7 (Ar, C=O, C=N). FT-IR ν(cm^{-1}) = 2929, 2859, 1739, 1643, 1587, 1431, 1335, 1267, 1191, 1127, 982, 962. Mass (FAB) *m*/*z* (rel. intensity) = 598 (87), 405 (100), 321 (60). Anal. Calcd. for $C_{35}H_{51}NO_7$: C 70.32, H 8.60, N 2.34; Found C 70.89, H 8.14, N 2.31%.

(4*S*)-4,5-Dihydro-4-[(*S*)-1-methylpropyl]-2-{4′-[3″,4″,5″-tris(hexyloxy)benzoyloxy]-2′-hydroxyphenyl}oxazole (2b). The general procedure gave **2b** as a colourless oil, yield 90%.

^{1}H NMR ($CDCl_3$, 300 MHz) 0.91 (m, 12H, CH_3), 0.97 (d, 3H, CH_3), 1.35, 1.49, 1.66, 1.80 (m, 27H, CH, CH_2), 4.04, 4.06 (t, 6H, OCH_2), 4.13, 4.24, 4.43 (m, 3H, oxazoline), 6.73, 6.86, 7.68 (m, 3H, inner Ar-H), 7.39 (s, 2H, outer Ar-H). ^{13}C NMR ($CDCl_3$, 75 MHz) 11.3, 14.0, 14.1, 14.8 (CH_3), 22.6, 22.7, 25.7, 25.9, 29.2, 30.3, 31.5, 31.7, 39.4 (CH, CH_2), 69.3, 69.6, 70.1, 73.6 (OCH_2, oxazoline), 108.2, 108.6, 110.1, 112.5, 123.6, 128.8, 143.1, 153.0, 154.8, 155.3, 161.2, 164.6 (Ar, C=O, C=N). FT-IR ν(cm^{-1}) = 2929, 2860, 1739, 1644, 1587, 1431, 1335, 1267, 1191, 1125, 982, 962. Mass (FAB) *m*/*z* (rel. intensity) = 640 (7), 406 (100), 322 (62). Anal. Calcd. for $C_{38}H_{57}NO_7$: C 71.33, H 8.98, N 2.19; Found C 72.09, H 10.22, N 2.19%.

(4*S*)-4,5-Dihydro-4-methyl-2-{4′-[3″,4″,5″-tris(dodecyloxy)benzoyloxy]-2′-hydroxyphenyl}oxazole (2c). The general procedure gave **2c** as a colourless waxy solid, yield 81%, mp 28 °C.

^{1}H NMR ($CDCl_3$, 300 MHz) 0.88 (t, 9H, CH_3), 1.37 (d, 3H, CH_3), 1.20–1.40, 1.50, 1.79 (m, 60H, CH_2), 4.03, 4.05 (t, 6H, OCH_2), 3.96, 4.46, 4.50 (m, 3H, oxazoline), 6.74, 6.87, 7.69 (m, 3H, inner Ar-H), 7.39 (s, 2H, outer Ar-H), 12.45 (s, 1H, OH). ^{13}C NMR ($CDCl_3$, 75 MHz) 14.1, 21.4 (CH_3), 22.6, 26.0, 29.3–29.7, 30.3, 31.9 (CH_2), 60.8, 69.2, 73.2, 73.5 (OCH_2, oxazoline), 108.6, 110.1, 112.5, 123.6, 128.8, 143.1, 152.9, 154.8, 161.1, 164.5 (Ar, C=O, C=N). FT-IR ν(cm^{-1}) = 2925, 2853, 1739, 1643, 1586, 1430, 1335, 1267, 1191, 1125, 982, 962. Mass (FAB) *m*/*z* (rel. intensity) = 851 (63), 658 (97), 490 (100). Anal. Calcd. for $C_{53}H_{87}NO_7$: C 74.87, H 10.31, N 1.65; Found C 74.69, H 10.17, N 1.61%.

(4*S*)-4,5-Dihydro-4-[(*S*)-1-methylpropyl]-2-{4′-[3″,4″,5″-tris(dodecyloxy)benzoyloxy]-2′-hydroxyphenyl}oxazole (2d). The general procedure gave **2d** as a waxy colourless solid, yield 93%, mp 39 °C.

^{1}H NMR ($CDCl_3$, 300 MHz) 0.88 (t, 9H, CH_3), 0.90 (d, 3H, CH_3), 0.96 (t, 3H, CH_3), 1.20–1.40, 1.49, 1.65, 1.79 (m, 63H, CH, CH_2), 4.04, 4.06 (t, 6H, OCH_2), 4.13, 4.24, 4.43 (m, 3H, oxazoline), 6.73, 6.87, 7.67 (m, 3H, inner Ar-H), 7.39 (s, 2H, outer Ar-H), 12.59 (s, 1H, OH). ^{13}C NMR ($CDCl_3$, 75 MHz) 11.3, 14.0, 14.7 (CH_3), 22.7, 26.1, 29.4–29.7, 30.3, 31.9, 39.3 (CH, CH_2), 69.3, 69.6, 70.1, 73.6 (OCH_2, oxazoline), 108.7, 110.1, 112.5, 123.7, 128.8, 143.2, 153.0, 154.8, 161.2, 164.5, 164.6 (Ar, C=O, C=N). FT-IR ν (cm^{-1}) = 2929, 2853, 1739, 1644, 1586, 1430, 1335, 1267, 1191, 1123, 981, 962. Mass (FAB) *m*/*z* (rel. intensity) = 893 (82), 658 (100), 490 (95). Anal. Calcd. for $C_{56}H_{93}NO_7$: C 75.36, H 10.50, N 1.57; Found C 75.13, H 10.48, N 1.55%.

(4*S*)-4,5-Dihydro-4-methyl-2-{4′-[3″,4″,5″-tris(dodecyloxy)benzoyloxy]phenyl}oxazole (2e). The general procedure gave **2e** as a colourless oil, which slowly crystallised, yield 73%.

^{1}H NMR ($CDCl_3$, 300 MHz) 0.88 (t, 9H, CH_3), 1.38 (d, 3H, CH_3), 1.15–1.40, 1.48, 1.78 (m, 60H, CH_2, CH_3), 3.98, 4.04, 4.06 (t, 6H, OCH_2), 4.41, 4.55 (m, 3H, oxazoline), 7.25, 8.02 (AA′BB′, 4H, inner Ar-H), 7.39 (s, 2H, outer Ar-H). ^{13}C NMR ($CDCl_3$, 75 MHz) 14.1, 21.4 (CH_3), 22.7, 26.1, 29.3–29.7, 30.3, 31.9 (CH_2), 62.1, 69.3, 73.6, 74.2 (OCH_2, oxazoline), 108.6, 121.8, 123.5, 125.5, 129.6, 143.1, 153.0, 153.4, 162.8, 164.6 (Ar, C=O, C=N). FT-IR ν(cm^{-1}) = 2920, 2851, 1740, 1649, 1587, 1335, 1196, 1120, 975, 939. Mass (FAB) *m*/*z* (rel. intensity) = 835 (100), 658 (63), 489 (35). Anal. Calcd. for $C_{53}H_{87}NO_6$: C 76.30, H 10.51, N 1.68; Found C 75.24, H 10.78, N 1.54%.

Bis{(4*S*)-4,5-dihydro-4-methyl-2-{4′-[3″,4″,5″-tris(hexyloxy)benzoyloxy]-2′-oxidophenyl-κ*O*}oxazole-κ*N*}palladium(II) (1a). The general procedure gave **1a** as a yellow solid, yield 70%, mp 72 °C (first heating).

^{1}H NMR ($CDCl_3$, 300 MHz) 0.91 (m, 18H, CH_3), 1.35, 1.48, 1.83 (m, 54H, CH_2, CH_3), 4.05 (m, 12H, OCH_2), 4.29, 4.53 (m, 6H, oxazoline), 6.42, 6.67, 7.64 (m, 6H, inner Ar-H), 7.38 (s, 4H, outer Ar-H). ^{13}C NMR ($CDCl_3$, 75 MHz) 14.0, 22.1 (CH_3), 22.6, 25.7, 29.2, 32.5 (CH_2), 57.2, 69.2, 73.5, 74.6 (OCH_2, oxazoline), 107.7, 108.5, 109.0, 113.2, 123.9, 130.4, 142.9, 152.9, 155.4, 161.5, 164.5, 168.9 (Ar, C=O, C=N). FT-IR ν(cm^{-1}) = 2929, 2859, 1732, 1621, 1586, 1539, 1428, 1335, 1267, 1191, 1132, 989, 957. Mass (FAB) *m*/*z* (rel. intensity) = 2001 (0.4), 1406 (0.2), 1298 (1), 321 (100). Anal. Calcd. for $C_{70}H_{100}N_2O_{14}Pd$: C 64.67, H 7.75, N 2.15; Found C 63.34, H 7.90, N 2.07%.

Bis{(4*S*)-4,5-dihydro-4-methyl-2-{4′-[3″,4″,5″-tris(dodecyloxy)benzoyloxy]-2′-oxidophenyl-κ*O*}oxazole-κ*N*}palladium(II) (1b). The general procedure gave **1b** as a greenish yellow waxy solid, yield 77%, mp 51 °C (first heating in DSC).

^{1}H NMR ($CDCl_3$, 300 MHz) 0.88 (t, 18H, CH_3), 1.26, 1.47, 1.78 (m, 126H, CH_2, CH_3), 4.03, 4.05 (t, 12H, OCH_2), 4.29, 4.57 (m, 6H, oxazoline), 6.42, 6.67, 7.64 (m, 6H, inner Ar-H), 7.37 (s, 4H, outer Ar-H). ^{13}C NMR ($CDCl_3$, 75 MHz) 14.1, 22.1 (CH_3), 22.7, 26.1, 29.3–29.7, 30.3, 31.9 (CH_2), 57.2, 69.3, 73.5, 74.6 (OCH_2, oxazoline), 107.7, 108.6, 109.0, 113.2, 123.9, 130.4, 143.0, 152.9, 155.4, 161.5, 164.5, 169.0 (Ar, C=O, C=N). FT-IR ν (cm^{-1}) = 2920, 2850, 1728, 1620, 1588, 1538, 1428,

1337, 1267, 1200, 1137, 990, 957. Mass (FAB) no signal could be obtained. Anal. Calcd. for $C_{106}H_{172}N_2O_{14}Pd$: C 70.54, H 9.60, N 1.55; Found C 70.47, H 9.56, N 1.56%

Bis{(4*S*)-4,5-dihydro-4-[(*S*)-1-methylpropyl]-{4′-[3″,4″,5″-tris-(dodecyloxy)benzoyloxy]-2′-oxidophenyl-κ*O*}oxazole-κ*N*}palladium(II) (1c). The general procedure gave **1c** as a greenish yellow waxy solid, yield 82%.

^{1}H NMR ($CDCl_3$, 300 MHz) 0.88 (m, 24H, CH_3), 1.02 (t, 6H, CH_3), 1.20–1.60, 1.80 (m, 120H, CH_2), 4.04, 4.05 (t, 12H, OCH_2), 4.42, 4.48, 4.62 (m, 6H, oxazoline), 6.39, 6.60, 7.61 (m, 6H, inner Ar-H), 7.38 (s, 4H, outer Ar-H). ^{13}C NMR ($CDCl_3$, 75 MHz) 11.9, 12.0, 14.1 (CH_3), 22.7, 26.1, 26.6, 29.3–29.7, 30.3, 31.9, 36.9 (CH_2, CH), 64.4, 68.4, 69.3, 73.6 (OCH_2, oxazoline), 107.6, 108.6, 109.0, 113.0, 124.0, 130.6, 143.0, 152.9, 155.4, 161.6, 164.4, 169.1 (Ar, C=O, C=N). FT-IR *v* (cm^{-1}) = 2923, 2852, 1735, 1624, 1588, 1539, 1428, 1335, 1256, 1194, 1129, 987, 946. Mass (FAB) *m*/*z* (rel. intensity) = 1888 (6), 996 (8), 893 (13), 658 (80), 490 (100). Anal. Calcd. for $C_{112}H_{184}N_2O_{14}Pd$: C 71.21, H 9.82, N 1.48; Found C 70.76, H 9.92, N 1.50%.

$Pd(OAc)_2L_2$ (L = (4*S*)-4,5-dihydro-2-{4′-[3″,4″,5″-tris(dodecyloxy)benzoyloxy]phenyl}-4-[(*S*)-1-methylpropyl]oxazole) (1m). The oxazoline ligand **2e** (0.3 mmol) was added to a hot solution of $Pd(OAc)_2$ (0.3 mmol) in acetic acid and the mixture was refluxed for 30 min to give a yellow solution, from which the crude product separated as a yellow oil. Recrystallisation from acetone at −10 °C gave a yellow solid, yield 67%.

^{1}H NMR (300 MHz, $CDCl_3$) 0.88 (t, 18H, CH_3), 1.22 (d, 6H, CH_3), 1.20–1.40, 1.49, 1.76, 1.86 (m, 120H, CH_2), 2.10 (s, 6H, CH_3(OAc)), 3.55, 3.95, 3.98 (m, 6H, oxazoline), 4.05 (t, 12H, OCH_2), 6.83, 6.92, 7.14 (m, 6H, inner Ar-H), 7.37 (m, 4H, outer Ar-H). ^{13}C NMR ($CHCl_3$) 14.1, 20.1, 24.1 (CH_3), 22.7, 26.1, 29.4–29.7, 30.3, 31.9 (CH_2), 57.5, 69.3, 73.6 (6C, OCH_2, oxazaline), 108.6, 117.5, 123.7, 124.7, 125.9, 129.0, 143.1, 149.1, 151.5, 153.0, 165.2, 172.7, 181.3 (Ar, C=O, C=N). FT-IR *v* (cm^{-1}) = 2925, 2853, 1728, 1633, 1584, 1573, 1335, 1195, 1178, 1117, 950, 934. Mass (FAB) no signal could be obtained. Anal. Calcd. for $C_{110}H_{178}N_2O_{16}Pd_2$: C 66.14, H 8.98, N 1.40; Found C 66.28, H 9.03, N 1.28%.

$PdCl_2L_2$ (L = (4*S*)-4,5-dihydro-2-{4′-[3″,4″,5″-tris(dodecyloxy)benzoyloxy]phenyl}-4-[(*S*)-1-methylpropyl]oxazole) (1n). To a stirred solution of the acetato-bridged complex **1m** (0.1 mmol) in CH_2Cl_2 was added a stoichiometric amount (3.45 ml, 0.058 M) of a solution of hydrogen chloride in methanol. The reaction mixture was stirred at ambient temperature for 12 h, the volume of the solution was reduced to 5 ml and acetone (30 ml) was added. The volume of the solution was again reduced to 10 ml and the product was crystallised at –10 °C to give yellow powdery crystals (61%), mp 64 °C (first heating in DSC).

^{1}H NMR ($CHCl_3$) 0.88 (t, 18H, CH_3), 1.00–1.50, 1.79 (m, 120H, CH_2), 1.47 (d, 6H, CH_3), 3.90–4.08 (m, 12H, OCH_2), 4.20–4.38, 4.68–4.82 (m, 6H, oxazoline), 6.91, 7.15, 7.22 (m, 6H, inner Ar-H), 7.28–7.42 (4H, outer Ar-H). ^{13}C NMR ($CHCl_3$) 14.1, 21.3 (CH_3), 22.7, 26.1, 29.3–29.7, 30.3, 31.9 (CH_2), 58.3, 69.3, 73.6 (OCH_2, oxazoline), 108.7, 118.5, 123.8, 126.2, 126.6, 128.2, 131.9, 143.1, 146.5, 151.6, 153.0, 164.6, 174.1 (Ar, C=O, C=N). FT-IR *v* (cm^{-1}) = 2923, 2852, 1731, 1631, 1580, 1336, 1183, 1118, 947. Mass (FAB) *m*/*z* (rel. intensity) = 2887 (4), 1914 (3), 1877 (3), 1771 (5), 835 (19), 658 (35), 489 (100). Anal. Calcd. for $C_{106}H_{172}Cl_2N_2O_{12}Pd_2$: C 65.28, H 8.89, N 1.44; Found C 65.30, H 8.95, N 1.36%.

Bis{(4*S*)-4,5-dihydro-4-methyl-2-{4′-[3″,4″,5″-tris(hexyloxy)-benzoyloxy]-2′-oxidophenyl-κ*O*}oxazole-κ*N*}nickel(II) (1d). The general procedure gave **1d** as a violet glassy solid, yield 62%.

^{1}H NMR ($CDCl_3$, 300 MHz) 0.90 (m, 18H, CH_3), 1.33, 1.47, 1.78 (m, 54H, CH_2, CH_3), 4.02, 4.04 (t, 12H, OCH_2), 4.15, 4.32, 4.40 (m, 6H, oxazoline), 6.32, 6.40, 7.50 (m, 6H, inner Ar-H), 7.35 (s, 4H, outer Ar-H). ^{13}C NMR ($CDCl_3$, 75 MHz) 14.0, 22.5 (CH_3), 22.6, 25.7, 29.2, 30.2, 31.5, 31.7 (CH_2), 55.6, 69.2, 73.5, 74.1 (OCH_2, oxazoline), 107.4, 108.4, 108.9, 113.7, 123.9, 128.9, 142.9, 152.9, 154.9, 163.1, 164.5, 166.7 (Ar, C=O, C=N). FT-IR *v* (cm^{-1}) = 2928, 2858, 1734, 1624, 1588, 1544, 1431, 1335, 1277, 1192, 1131, 989, 959. Mass (FAB) *m*/*z* (rel. intensity) = 1905 (3), 1273 (9), 405 (21), 321 (100). Anal. Calcd. for $C_{70}H_{100}N_2O_{14}Ni$: C 67.14, H 8.05, N 2.24; Found C 67.42, H 8.40, N 2.34%.

Bis{(4*S*)-4,5-dihydro-4-[(*S*)-1-methylpropyl]-2-{4′-[3″,4″,5″-tris-(hexyloxy)benzoyloxy]-2′-oxidophenyl-κ*O*}oxazole-κ*N*}nickel(II) (1e). The general procedure gave **1e** as a violet solid, yield 99%, mp 90 °C (first heating).

^{1}H NMR ($CDCl_3$, 300 MHz) 0.90 (t, 18H, CH_3), 0.98 (t, 6H, CH_3), 1.07 (d, 6H, CH_3), 1.33, 1.47, 1.77 (m, 52H, CH_2), 4.03, 4.04 (t, 12H, OCH_2), 4.09, 4.26, 4.32 (m, 6H, oxazoline), 6.30, 6.35, 7.46 (m, 6H, inner Ar-H), 7.35 (s, 4H, outer Ar-H). ^{13}C NMR ($CDCl_3$, 75 MHz) 12.0, 12.1, 13.9, 14.0 (CH_3), 22.5, 22.6, 25.6, 25.7, 26.6, 29.2, 30.2, 31.5, 31.6, 37.5 (CH_2, CH), 62.7, 67.9, 69.1, 73.5 (OCH_2, oxazoline), 107.2, 108.4, 108.7, 113.4, 123.9, 129.1, 142.8, 152.8, 154.8, 162.7, 164.4, 166.9 (Ar, C=O, C=N). FT-IR *v* (cm^{-1}) = 2930, 2859, 1734, 1625, 1588, 1544, 1432, 1336, 1278, 1194, 1129, 987. Mass (FAB) *m*/*z* (rel. intensity) = 2031 (51), 1392 (22), 1358 (17), 1335 (13), 640 (100). Anal. Calcd. for $C_{76}H_{112}N_2O_{14}Ni$: C 68.30, H 8.45, N 2.10; Found C 68.28, H 8.54, N 2.18%.

Bis{(4*S*)-4,5-dihydro-4-methyl-2-{4′-[3″,4″,5″-tris(dodecyloxy)-benzoyloxy]-2′-oxidophenyl-κ*O*}oxazole-κ*N*}nickel(II) (1f). The general procedure gave **1f** as a violet waxy solid, yield 48%, mp 69 °C.

^{1}H NMR ($CDCl_3$, 300 MHz) 0.88 (t, 18H, CH_3), 1.48 (d, 18H, CH_3), 1.15–1.40, 1.46, 1.77 (m, 120H, CH_2), 4.02, 4.04 (t, 12H, OCH_2), 4.09, 4.15, 4.41 (m, 6H, oxazoline), 6.32, 6.39, 7.49 (m, 6H, inner Ar-H), 7.35 (s, 4H, outer Ar-H). ^{13}C NMR ($CDCl_3$, 75 MHz) 14.0, 22.4 (CH_3), 22.6, 26.0, 29.3–29.7, 30.3, 31.9 (CH_2), 55.4, 69.3, 73.5, 74.0 (OCH_2, oxazoline), 107.4, 108.6, 108.9, 113.6, 123.9, 128.9, 143.0, 152.9, 154.9, 162.8, 164.5, 166.8 (Ar, C=O, C=N). FT-IR *v* (cm^{-1}) = 2923, 2853, 1733, 1623, 1587, 1543, 1431, 1335, 1279, 1194, 1130, 991, 960. Mass (FAB) *m*/*z* (rel. intensity) 2664 (4), 1779 (19), 1757 (7), 851 (24), 658 (67), 490 (100). Anal. Calcd. for $C_{106}H_{172}N_2O_{14}Ni$: C 72.45, H 9.87, N 1.59; Found C 73.13, H 10.12, N 1.56%.

Bis{(4*S*)-4,5-dihydro-4-[(*S*)-1-methylpropyl]-2-{4′-[3″,4″,5″-tris-(dodecyloxy)benzoyloxy]-2′-oxidophenyl-κ*O*}oxazole-κ*N*}nickel-(II) (1g). The general procedure gave **1g** as a violet oil, yield 75%.

^{1}H NMR ($CDCl_3$, 300 MHz) 0.88 (t, 18H, CH_3), 0.98 (t, 6H, CH_3), 1.07 (d, 6H, CH_3), 1.15–1.40, 1.46, 1.77 (m, 120H, CH_2), 4.02, 4.04 (t, 12H, OCH_2), 4.11, 4.26, 4.33 (m, 6H, oxazoline), 6.30, 6.35, 7.46 (m, 6H, inner Ar-H), 7.35 (s, 4H, outer Ar-H). ^{13}C NMR ($CDCl_3$, 75 MHz) 12.0, 12.1, 14.1 (CH_3), 22.6, 26.0, 26.6, 29.3–29.7, 30.3, 31.9, 37.5 (CH_2, CH), 55.2, 62.8, 69.3, 73.6 (OCH_2, oxazoline), 107.2, 108.6, 108.8, 113.5, 123.9, 129.1, 143.0, 152.9, 154.9, 162.8, 164.4, 166.9 (Ar, C=O, C=N). FT-IR *v* (cm^{-1}) = 2924, 2853, 1734, 1624, 1588, 1545, 1432, 1336, 1277, 1194, 1128, 987, 948. Mass (FAB) *m*/*z* (rel. intensity) = 2788 (3), 1840 (8), 893 (57), 658 (84), 490 (100). Anal. Calcd. for $C_{112}H_{184}N_2O_{14}Ni$: C 73.05, H 10.07, N 1.52; Found C 73.08, H 9.98, N 1.51%.

Bis{(4*S*)-4,5-dihydro-4-methyl-2-{4′-[3″,4″,5″-tris(hexyloxy)-benzoyloxy]-2′-oxidophenyl-κ*O*}oxazole-κ*N*}copper(II) (1h). The general procedure gave **1h** as a green glassy solid, yield 99%.

FT-IR ν (cm^{-1}) = 2928, 2858, 1734, 1622, 1587, 1542, 1430, 1335, 1275, 1192, 1129, 986, 958. Mass (FAB) *m/z* (rel. intensity) = 1917 (1), 1318 (5), 1064 (2), 722 (2), 660 (7), 405 (23), 321 (100). Anal. Calcd. for $C_{70}H_{100}N_2O_{14}Cu$: C 66.88, H 8.02, N 2.23; Found C 67.22, H 7.99, N 2.21%.

Bis{(4*S*)-4,5-dihydro-4-methyl-2-{4′-[3″,4″,5″-tris(dodecyloxy)-benzoyloxy]-2′-oxidophenyl-κ*O*}oxazole-κ*N*}copper(II) (1i). The general procedure gave **1i** as green crystals in 69% yield, mp 88 °C.

FT-IR ν (cm^{-1}) = 2923, 2853, 1737, 1621, 1589, 1542, 1431, 1335, 1275, 1194, 1130, 986, 957. Mass (FAB) *m/z* (rel. intensity) = 2675 (7), 1824 (8), 1785 (6), 1763 (5), 1569 (6), 913 (25), 658 (37), 490 (100). Anal. Calcd. for $C_{106}H_{172}N_2O_{14}Cu$: C 72.25, H 9.84, N 1.59; Found C 72.27, H 9.83, N 1.58%.

Bis{(4*S*)-4,5-dihydro-4-[(*S*)-1-methylpropyl]-2-{4′-[3″,4″,5″-tris-(dodecyloxy)benzoyloxy]-2′-oxidophenyl-κ*O*}oxazole-κ*N*}copper-(II) (1j). The general procedure gave **1j** as a green glassy solid in 70% yield.

FT-IR ν (cm^{-1}) = 2925, 2854, 1736, 1624, 1587, 1542, 1432, 1335, 1275, 1260, 1194, 1127, 986, 948. Mass (FAB) *m/z* (rel. intensity) = 2800 (3), 1908 (4), 1846 (3), 1612 (3), 955 (19), 658 (34), 490 (100). Anal. Calcd. for $C_{112}H_{184}N_2O_{14}Cu$: C 72.86, H 10.04, N 1.52; Found C 72.82, H 10.00, N 1.52%.

Bis{(4*S*)-4,5-dihydro-4-methyl-2-{4′-[3″,4″,5″-tris(dodecyloxy)-benzoyloxy]-2′-oxidophenyl-κ*O*}oxazole-κ*N*}zinc(II) (1k). The general procedure gave **1k** as a colourless solid in 83% yield, mp 94 °C.

^{1}H NMR ($CDCl_3$, 300 MHz) 0.86 (t, 18H, CH_3), 1.34 (d, 6H, CH_3), 1.00–1.40, 1.45, 1.77 (m, 120H, CH_2), 4.04, 4.05 (t, 12H, OCH_2), 4.45, 4.61 (m, 6H, oxazoline), 6.44, 6.67, 7.74 (m, 6H, inner Ar-H), 7.39 (s, 4H, outer Ar-H). ^{13}C NMR ($CDCl_3$, 75 MHz) 14.1, 21.5 (CH_3), 22.7, 26.1, 29.3–29.7, 30.3, 31.9 (CH_2), 59.7 (CH oxazoline), 72.7 (CH_2 oxazoline), 69.2, 73.5 (OCH_2), 108.5, 108.7, 115.0, 131.2 [tert. C(Ar)], 107.1, 124.0, 142.9, 152.9, 156.7, 164.5, 169.1, 171.6 [quart. C(Ar), C=O, C=N]. FT-IR ν (cm^{-1}) = 2924, 2852, 1727, 1621, 1586, 1546, 1430, 1335, 1275, 1196, 1123, 986, 957. Mass (FAB) no signal could be obtained. Anal. Calcd. for $C_{106}H_{172}N_2O_{14}Zn$: C 72.18, H 9.83, N 1.59; Found C 72.14, H 9.97, N 1.68%.

Bis{(4*S*)-4,5-dihydro-4-[(*S*)-1-methylpropyl]-2-{4′-[3″,4″,5″-tris-(dodecyloxy)benzoyloxy]-2′-oxidophenyl-κ*O*}oxazole-κ*N*}zinc(II) (1l). The general procedure gave **1l** as a colourless solid in 75% yield, mp 55 °C.

^{1}H NMR ($CDCl_3$, 300 MHz) 0.85 (m, 30H, CH_3), 1.10–1.40, 1.48 1.78 (m, 120H, CH_2), 4.03, 4.04 (t, 12H, OCH_2), 4.25, 4.40 (m, 6H, oxazoline), 6.42, 6.75, 7.72 (m, 6H, inner Ar-H), 7.38 (s, 4H, outer Ar-H). ^{13}C NMR ($CDCl_3$, 75 MHz) 11.6, 12.5, 14.1 (CH_3), 22.7, 26.1, 26.6, 29.3–29.7, 30.3, 31.9, 37.7 (CH_2, CH), 66.9, 67.8, 69.2, 73.5 (OCH_2, oxazoline), 107.2, 108.5, 115.1, 124.0, 131.2, 142.8, 152.9, 156.6, 164.5, 169.2, 171.6 (Ar, C=O, C=N). FT-IR ν (cm^{-1}) = 2921, 2851, 1738, 1621, 1589, 1538, 1428, 1336, 1273, 1198, 1116, 989, 947. Mass (FAB) *m/z* (rel. intensity) = 1847 (2), 893 (19), 658 (44), 489 (100), 321 (37). Anal. Calcd. for $C_{112}H_{184}N_2O_{14}Cu$: C 72.79, H 10.03, N 1.52; Found C 72.88, H 10.13, N 1.62%.

Acknowledgement

This work was supported by the C.I.C.Y.T. (Projects: MAT1999-1009-CO2-02 and MAT2000-1293-CO2-01) and by the European Project FMRX-CT97-0121 (Dr M. Lehmann's fellowship).

References

1 N. Boden and B. Movaghar, in *Handbook of Liquid Crystals*, Vol. 2B, Wiley-VCH, Weinheim, 1998, pp. 781–798.
2 J. L. Serrano, T. Sierra, Y. González, C. Bolm, K. Weickhardt, A. Magnus and G. Moll, *J. Am. Chem. Soc.*, 1995, **117**, 8312–8321.
3 M. Lehmann, M. Marcos, J. L. Serrano, T. Sierra, C. Bolm, K. Weickhardt, A. Magnus and G. Moll, *Chem. Mater.*, 2001, **13**, 4374–4381.
4 H.-T. Nguyen, C. Destrade and J. Malthête, *Adv. Mater.*, 1997, **9**, 375–388.
5 (*a*) H. Bock and W. Helfrich, *Liq. Cryst.*, 1992, **12**, 697–703; (*b*) H. Bock and W. Helfrich, *Liq. Cryst.*, 1995, **18**, 387–399; (*c*) H. Bock and W. Helfrich, *Liq. Cryst.*, 1995, **18**, 707–713; (*d*) G. Heppke, D. Krüerke, M. Müller and H. Bock, *Ferroelectrics*, 1996, **179**, 203–209; (*e*) G. Scherowsky and X. H. Chen, *Liq. Cryst.*, 1994, **17**, 803–810; (*f*) G. Scherowsky and X. H. Chen, *J. Mater. Chem.*, 1995, **5**, 417–421; (*g*) J. L. Serrano and T. Sierra, *Chem Eur. J.*, 2000, **6**, 759–766.
6 (*a*) C. Bolm, K. Weickhardt, M. Zehnder and D. Glasmacher, *Helv. Chim. Acta*, 1991, **74**, 717–726; (*b*) C. Bolm, K. Weickhardt, M. Zehnder and T. Ranff, *Chem. Ber.*, 1990, **124**, 1173–1180; (*c*) M. Gómez, G. Muller and M. Rocamora, *Coord. Chem. Rev.*, 1999, **193–195**, 769–835.
7 (*a*) M. B. Ros, N. Ruiz, J. L. Serrano and P. Espinet, *Liq. Cryst.*, 1991, **9**, 77–86; (*b*) J. Barberá, P. Espinet, E. Lalinde, M. Marcos and J. L. Serrano, *Liq. Cryst.*, 1987, **2**, 833–842.
8 W. Seeliger, E. Aufderhaar, W. Diepers, R. Feinauer, R. Nehring, W. Thier and H. Hellmann, *Angew. Chem.*, 1966, **78**, 913–927.
9 (*a*) H. Ringsdorf, R. Wüstefeld, E. Zerta, M. Ebert and J. H. Wendorff, *Angew. Chem., Int. Ed. Engl.*, 1989, **101**, 934; 1989, **28**, 914; (*b*) M. M. Green, H. Ringsdorf, J. Wagner and R. Wüstefeld, *Angew. Chem.*, 1990, **102**, 1525–1528*Angew. Chem. Int. Ed. Engl.1990,* **29**, 1478–1481 (see also the cited literature in refs 7 and 8).
10 I. D. Fletcher, D. Guillon, B. Heinrich, A. Omenat and J. L. Serrano, *Liq. Cryst.*, 1997, **23**, 51–58.
11 T. Hegmann, J. Kain, S. Diele, G. Pelzl and C. Tschierske, *Angew. Chem., Int. Ed.*, 2001, **40**, 887–890.
12 I. Letko, S. Diele, G. Pelzl and W. Weissflog, *Mol. Cryst. Liq. Cryst.*, 1995, **260**, 171–183.
13 P. Espinet, J. Pérez, M. Marcos, M. B. Ros, J. L. Serrano, J. Barberá and A. M. Levelut, *Organometallics*, 1990, **9**, 2028–2033.
14 P. G. de Gennes, *The Physics of Liquid Crystals*,Clarendon, Oxford, 3rd edn., 1982.
15 (*a*) J.-C. Martin and R. Cano, *C. R. Acad. Sci., Ser. B*, 1974, **278**, 219–22; (*b*) G. Heppke and F. Oestreicher, *Z. Naturforsch., A*, 1997, **32**, 899–901.
16 F. Meyer, K. Siemensmeyer, K.-H. Etzbach and P. Schuhmacher, *Int. Pat.* WO 97/00600, 1995.